Study on Accuracy Improvement of Registration for Transcranial Magnetic Stimulation

Se-jong Ahn, Sung-wook Shin, Hyu-jeong Kim and Sung-taek Chung

Dept of computer Engineering, Korea Polytechnic University, Postal Code 429-793, Siheung, Korea

Se-jin Yoon

CRTechnology Co., Ltd., Daejeon, Korea

Summary
Transcranial Magnetic Stimulation (TMS) is a noninvasive method using magnetic simulation and is being used for stroke patients or those with various cerebral diseases accompanying memory impairment, such as Parkinson's disease and depression. This type of treatment is to stimulate the brain directly, and it is essential to apply correct stimulation to an anatomical position of a patient. For effective TMS, therefore, a navigation system is needed to provide information about a correct position for stimulation. This system shows the location and the direction of the stimulated position on the three-dimensional magnetic resonance imaging of a patient and applies magnetic stimulation to a correct location in consideration of anatomical features of individual patients. To apply such a navigation system, technology for tracing a relative coordinate of a transducer that generates a magnetic field is necessary to stimulate the brain and the head location of a patient. For the real-time tracing of the coordinate, therefore, this study used two cameras to draw a three-dimensional coordinate through view-difference algorithm of the cameras, analytical forward intersection, camera calibration, and information about internal elements of the cameras. A program was developed to show registration between information about the head location and posture of a patient through the three-dimensional coordinate and the three-dimensional model obtained from the magnetic resonance imaging data in real time.

Key words:
Transcranial Magnetic Stimulation(TMS), Field of View(FOV), Navigation System, Registration, Camera Calibration,

1. Introduction

With the aging population, the increase in stroke has become an important problem in the socio-economic respect. Stroke is the second most frequent cause of death, following cancer, and accounts for 13.9% of all the causes of death and is on the continuous increase [1].

In the research on stroke, a transcranial magnetic stimulation system is used as a tool to assess the degree of damage to the brain functions and their recovery. This system was introduced by Barker and his colleagues 1985 to solve the problem of causing discomfort and pain to a patient [2]. After its introduction, the increasing concern about transcranial magnetic stimulation led to other techniques, including repetitive transcranial magnetic stimulation. These continuous magnetic stimulation techniques are applied to diverse clinical diseases, such as stroke, depression, Parkinson's disease, and epilepsy, through activation of cortical neurons by using evoked potential [3-4]. The combined use of transcranial magnetic stimulation and functional neuroimaging is reportedly very effective in examining functional association among brain areas. Recently a navigation system is frequently applied to stimulate the head of a patient effectively in a transcranial magnetic stimulation system [5]. While a general TMS system cannot focus on the location for actual stimulation because even stimulation of the same location doesn't enable one to position the position for stimulation, a navigation system can visualize where a magnetic field stimulates in the brain, thus making it possible to apply magnetic stimulation to the desired magnetic position [6].

Figure 1 demonstrates a TMS navigation system in actual use by registering the location of the head of a patient and that of the three-dimensional model implemented through magnetic resonance imaging, identifying where the magnetic field of a transducer stimulates in the brain through software, and applying stimulation directly to the head of the patient for treatment, and Figure 2 shows a block diagram of the TMS navigation system.

Fig. 1 TMS Navigation System

Manuscript received February 5, 2012
Manuscript revised February 20, 2012

One of the most important parts in this navigation system is the process of registering three-dimensional modeling through magnetic resonance imaging and the photographed head location of the patient. It is necessary to set a coordinate in the three-dimensional model of a patient's head, place a reflective marker on what is the coordinate set on the actual head of the patient, and register the coordinate on the software and that on the patient's head [7]. Figure 3 shows a navigation system for registration between the three-dimensional model on software and the actual head of a patient, with the red dot representing the location of marker for the three-dimensional model on software and the blue dot representing the location shown by imaging of the marker which is directly attached to the defined location and induced by a camera. Perfect registration of the red and blue dots makes the three-dimensional model on software move when a patient's movement is captured by a camera. In this process, poor registration can make the actually stimulated location differ from the stimulated location shown on software and increase errors, consequently resulting not only in poor cerebral magnetic stimulation rehabilitation treatment but also in damage to the patient's health if worst [8]. Therefore, an algorithm whose errors are smaller than others is needed, and it is also necessary examine the factors affecting errors in camera performance and location.

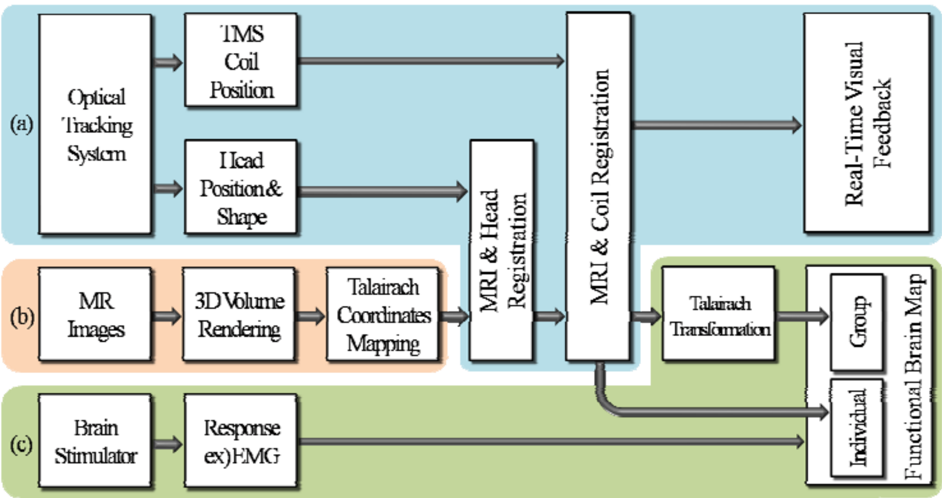

Fig. 2 The outline of the transcranial magnetic stimulation navigation system. (a) Tracking and registration using optical tracking system. (b) 3D volume rendering of MRI and Talairach coordinates mapping. (c) Functional brain mapping for the response of brain stimulation.

This study considered reducing the differences between the three-dimensional coordinate obtained through a camera by using analytical forward intersection and that obtained through magnetic resonance imaging to use a navigation system. An attempt was made to see how such factors as camera calibration, resolution, and baseline, or the distance between cameras were associated with coordinate errors and determine how these factors affected the field of view (FOV), which is the space for photographing.

2. Methodology

2.1 Forward Intersection

Forward intersection refers to the method of using an image coordinate of a camera to induce the three-dimensional location of the object [9]. Forward intersection is divided into forward intersection using collinearity equation and analytical forward intersection. Forward intersection using collinearity equation is in universal use, but is somewhat complicated and relatively time-consuming since it uses matrix multiplication and inverse-matrix operation. For this reason, analytical forward intersection was used to make smooth real-time coordinate tracing.

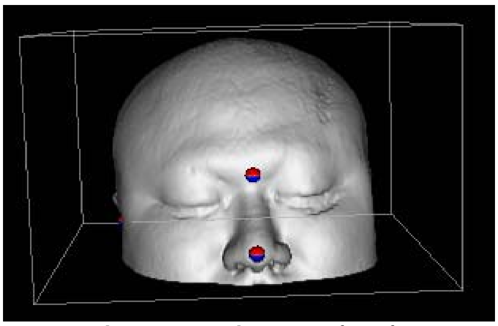

Fig. 3 The Registration between surface of patient and three-dimensional model on application

Analytical forward intersection is to calculate the distance between the object and that made by right and left cameras and define the three-dimensional location of the object

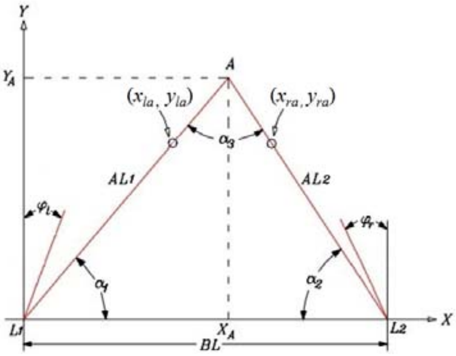

Fig. 4 Forward Intersection

A = target, L_1 = left camera, L_2 = right camera
X_A = X coordinate of target, Y_A = Y coordinate of target
x_{la} = X coordinate of target at left camera (pixel)
x_{ra} = X coordinate of target at right camera(pixel)
y_{la} = Y coordinate of target at left camera (pixel)
y_{ra} = Y coordinate of target at right camera(pixel)
BL(baseline)=distance between two cameras
φ_l = angle between left camera and baseline
φ_r = angle between right camera and baseline
AL_1= distance from left camera to target
AL_2= distance from right camera to target
α_1= angle between AL_1 and baseline
α_2= angle between AL_2 and baseline
α_3= angle between AL_1 and AL_2

Figure 4 shows analytical forward intersection using an image coordinate. The left angle φ_l and the right angle φ_r refer to the angles the camera rotated around the baseline (BL): 0° for the Y-axis direction and -90° for the X-axis direction. x_{la} and x_{ra} refer to the coordinates of the object found in the image of each camera. Focus length of camera f can be used to determine the relations between cameras and the object in real space, and the results α_1 and α_2 can be used to determine the length of AL_1 and AL_2 (e.g., see Eq. 1).

$$\begin{aligned}
\alpha_1 &= 90^\circ + \varphi_l - \tan^{-1}\left(\frac{x_{la}}{f}\right) \\
\alpha_2 &= 90^\circ - \varphi_r + \tan^{-1}\left(\frac{x_{ra}}{f}\right) \\
\alpha_3 &= 180^\circ - \alpha_1 - \alpha_2 \\
AL_1 &= BL \times \frac{\sin\alpha_2}{\sin\alpha_3} \\
AL_2 &= BL \times \frac{\sin\alpha_1}{\sin\alpha_3}
\end{aligned} \tag{1}$$

In the coordinate system based on the left camera, coordinates X_A and Y_A in real space can be estimated with the sides and angles of the triangle formed by two cameras and the object. As Z_A is coordinates of Z to show height of target, Z_A can be estimated by applying forward distance from the object in comparison with the focus length to the mean of the y_{la} and y_{ra} coordinates from left and right cameras, respectively (e.g., see Eq. 2).

$$\begin{aligned}
X_A &= \frac{AL_1 \times \cos\alpha_1 + BL - AL_2 \times \cos\alpha_2}{2} \\
Y_A &= \frac{AL_1 \times \sin\alpha_1 + AL_2 \times \sin\alpha_2}{2} \\
Z_A &= \frac{y_{la} + y_{ra}}{2} \times \frac{Y_A}{f}
\end{aligned} \tag{2}$$

Figure 5 shows real-time location of the reflective marker by software tracing the three-dimensional coordinate of the marker as mentioned above. As shown in the Figure 5, coordinates of the reflective marker vary according to the location of the camera. The value of the three-dimensional coordinate for the reflective marker can be determined by the differences in coordinates between the two images.

Fig. 5 Application to trace the three-dimensional coordinate at two camera images

2.2 Calibration & Distortion

In general, cameras have different internal elements, including focus length and lens distortion. These features of cameras vary significantly by the differences in their internal factors in case of the same kind of cameras; such variation affects determination of the correct three-dimensional location from imaging. Therefore, camera calibration for determining internal elements of a camera to make more accurate measurements is needed. This study used Zhang's calibration to determine internal variables of cameras [10].

GML Camera Calibration Tool Box was used to determine internal elements of cameras. Calibration pattern images photographed from different locations and angles were analyzed to determine internal elements and distortion coefficients of cameras. Figure 6 shows determination of the apex in each box of the chessboard in GML Camera Calibration Tool Box; the distortion rate of cameras can be estimated on the basis of the location of each apex.

$$\begin{aligned}
&Square\ size = one\ square\ \ size\ of\ \ chessboard\\
&Focal\ length = distance\ \ from\ center\ of\ \ lens\ to\ \ focus\\
&Principal\ \ Point = the\ points\ where\ the\ principal\ planes\\
&\qquad\qquad\qquad cross\ the\ optical\ axis\\
&Distortion = distortion\ rate,[K1, K2, P1, P2]\\
&K1, K2 = radial\ \ distortion\\
&P1, P2 = tangential\ \ distortion
\end{aligned}$$

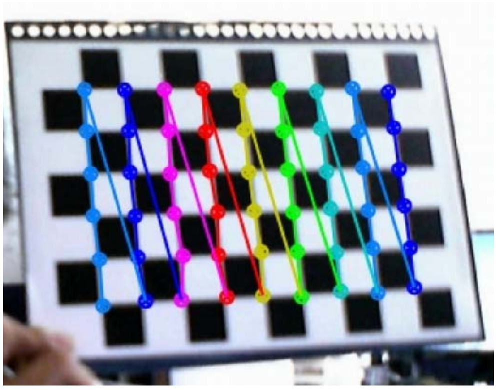

Fig. 6 shows the camera calibration test

Number of images	301
Square size	22,100 (mm)
Focal length	[1455,200 1458,364] ± [1,643 1,621]
Principal point	[524,506 296,286] ± [1,107 0,960]
Distortion	[-0,180354 0,001974 0,001716 -0,000194] ± [0,001016 0,002699 0,000088
The camera matrix	[1455,200 0 524,506; 0 1458,364 296,286; 0 0 1]
Pixel error	[0,32 0,24]

Fig. 7 Results of calibration operations with the points

Figure 7 shows the results of calibration operations with the points. The CCD camera used for the operations is AlphaCam C-3000 with resolution of 1280 * 720 and the angle of view of 66.5˚. Figure 7 shows focal length and the principal point of the camera on the screen. Four parameters of distortion refer to K1 and K2 radial distortion and P1 and P2 tangential distortion, respectively. Since the photographed picture is distorted from the real world by the lens, it is necessary to be undistorted. This can be undistorted by substituting four distortion coefficients obtained through camera calibration for the following equation 3 (e.g., see Eq. 3) [11-12].

$$\begin{aligned}
x_u &= (1+\sum_{i=1}^{\infty} K_i r^{2i})x_d + (2P_1\overline{xy} + P_2(r^2 + 2\overline{x^2}))(1+\sum_{i=1}^{\infty} P_{i+2} r^{2i}) \qquad (3)\\
y_u &= (1+\sum_{i=1}^{\infty} K_i r^{2i})y_d + (P_1(r^2 + 2\overline{y^2}) + 2P_2\overline{xy})(1+\sum_{i=1}^{\infty} P_{i+2} r^{2i})\\
x_u &= (1+K_1 r^2 + k_2 r^4)x_d + (2P_1\overline{xy} + P_2(r^2 + 2\overline{x^2}))\\
x_u &= (1+K_1 r^2 + k_2 r^4)y_d + (P_1(r^2 + 2\overline{y^2}) + 2P_2\overline{xy})
\end{aligned}$$

$$\begin{aligned}
&\overline{x} = x_d - C_x\\
&\overline{y} = y_d - C_y\\
&r_2 = \overline{x_2} + \overline{y_2}\\
&C_x, C_y = optical\ \ center\\
&K_i = radial\ \ distortion\\
&P_i = tangential\ \ distortion\\
&x_d = x - coordinate\ before\ undistortion\\
&y_d = y - coordinate\ before\ undistortion\\
&x_u = x - coordinate\ after\ undistortion\\
&y_u = y - coordinate\ after\ undistortion
\end{aligned}$$

Figure 8 shows comparison between before and after undistortion. (a) shows the image before undistortion, with the edge bent. (b) shows the image after undistortion, with the edge bending undistorted.

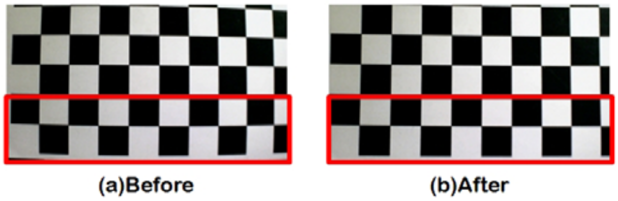

Fig. 8 Result of undistortion image, (a) is distorted image and (b) is undistorted image

2.3 Baseline

Baseline is one of the most important external elements of cameras and directly affects accuracy of range measurement. In general, greater baseline leads to greater differences of view from the same range between both cameras, less changes in the range with increased differences of view, and higher range resolution on the basis of the view differences [13]. Correlation between range Y and disparity on the basis of baseline is as follows (e.g., see Eq. 4).

$$Y = BL\sqrt{(Resolution of\ X / Disparity)^2 - 1} \qquad (4)$$

Therefore, longer baseline leads to higher precision. However, since an increase in baseline shortens the minimum measurement range, medical practice with restricted space requires suggestions of proper baseline and FOV.

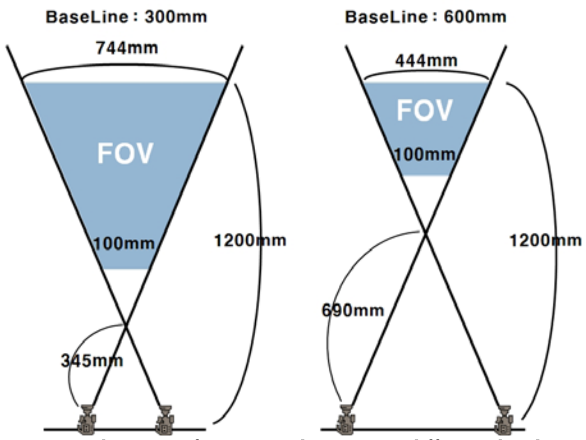

Fig. 9 The Space of FOV according to twice difference baseline

Figure 9 shows the changing features of FOV when the baseline increases from 300mm to 600mm. Here, the angle of view for the camera is 66.5˚. In general, greater baseline leads to narrower short-distance FOV. If FOV has the marginal measurement range of 1200mm and the minimum measurement width of 100mm, the baseline of 300mm leads to 345mm of intersection for camera image and 744mm of width for the marginal measurement range, while the baseline of 600mm leads to 690mm of intersection for camera image and as narrow as 444mm of width for the marginal measurement range. The greater baseline, the smaller errors but the smaller area of FOV; it is therefore necessary to expand the baseline to improve precision at the level not restricting space usability in medical practice and consider security of FOV not disturbing the use of a TMS navigation system

3. Experimental Results

3.1 Analytical Forward Intersection

Equations 1 and 2 were applied to determine how much analytical forward intersection reflecting mechanical features could reduce errors as compared with simple triangulation, the results of which are shown in Figure 9. The camera used in this process is AlphaCam C-3000 with resolution of 1280 * 720 pixel, the angle of view of 66.5˚, and the baseline, or the distance between two cameras, of 300mm.

Figure 10 presents the results of triangulation in the solid line and those of analytical forward intersection in the dotted line. As shown in the figure, the errors of triangulation are approximately 1.37 times larger than those of analytical forward intersection. This is because unlike general triangulation, analytical forward intersection revises the focus length within the camera before estimation and has the focus length improve accuracy in conversion into the distance of actual space, thereby making smaller errors.

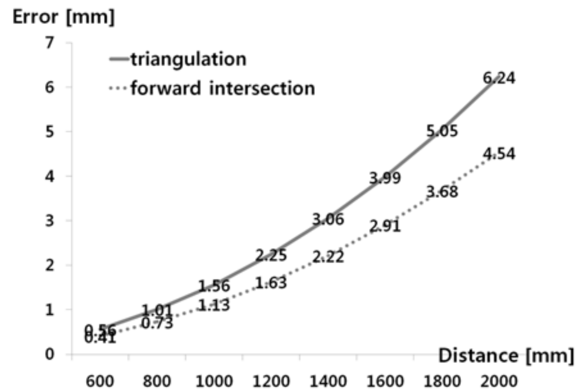

Fig. 10 Comparisons between the errors of triangulation and forward intersection

3.2 Undistortion

Equation 3 was applied to determine how the errors occurring at the edge of the photographed image due to distortion features of the lens differed from those in the undistorted image. The camera used in this process is also AlphaCam C-3000 with resolution of 1280 * 720 pixels, the angle of view of 66.5˚, and distortion values of image without undistortion as shown in Figure 7.

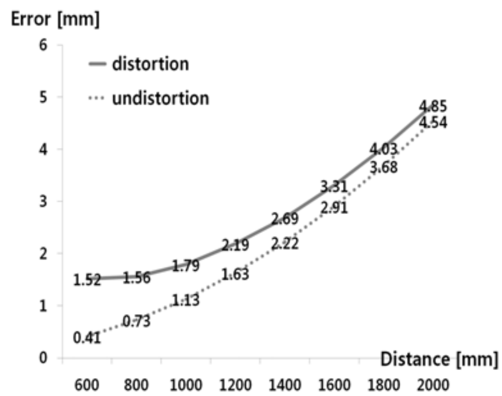

Fig. 11 Comparisons between the errors of distortion and undistortion

Figure 11 presents the errors for image not going through undistortion in the solid line and those for undistorted image in the dotted line. Longer range leads to smaller errors caused by undistortion because there are more errors due to the range and distortion values than those caused by quantization errors.

3.3 Resolution and Baseline

Other factors involved in reducing errors of a three-dimensional coordinate include resolution and baseline, which is the distance between two cameras. In general, higher resolution leads to smaller errors due to quantization errors during the conversion of an analogue image to a digital image. To confirm this, comparison was made for errors on the basis of resolution between two types of cameras, which is shown in Table 1. The cameras used in this process are AlphaCam C-3000 with 1280*720 pixel and Logitech Webcam C120 with 640*480, with the angle of view of 66.5˚ and 62˚, respectively. Analytical forward intersection uses width of a camera image as a formula using triangulation of two cameras. Therefore, since there is twice difference in resolution between two cameras, the errors must be different twice according to equations 1 and 2. However, the errors of the actual image differ by approximately 2.17 times because different angles of view for the two cameras lead to different width of images.

Greater baseline leads to greater differences of view to the same range for both cameras, which means a decrease in the range presented by each disparity. Therefore, precision for the same range increases. To confirm this, the same AlphaCam C-3000 camera was placed in a different way to compare the errors due to a change in the baseline, which is shown in Table 2. As the baseline doubles from 300mm to 600mm, the errors decrease to a half.

Table 1: Error on the basis of resolution between two types camera ***(BL 300mm)***

Distance	*640*480pixel*	*1280*720pixel*
600 mm	0.886 mm	0.408 mm
800 mm	1.576 mm	0.726 mm
1000 mm	2.464 mm	1.134 mm
1200 mm	3.549 mm	1.633 mm
1400 mm	4.834 mm	2.223 mm
1600 mm	6.317 mm	2.905 mm
1800 mm	7.999 mm	3.677 mm
2000 mm	9.880 mm	4.541 mm

Table 2: Error on the basis of baseline between two camera ***(Resolution 1280*720)***

Distance	*BL 300mm*	*BL 600mm*
1000 mm	1.134	0.566
1200 mm	1.633	0.816
1400 mm	2.223	1.111
1600 mm	2.905	1.451
1800 mm	3.677	1.837
2000 mm	4.541	2.268

4. Conclusion

This study intended to make registration between the three-dimensional coordinate obtained through images from two cameras and that obtained through magnetic resonance imaging. Triangulation in general use is frequently utilized due to a simple measurement algorithm but had too great errors to be applied to a TMS navigation system. Therefore, analytical forward intersection was used for application to the TMS navigation system, and calibration and undistortion were carried out to reduce errors of a camera itself. Besides, an attempt was made to analyze the error range according to the differences in the baseline and determine correlation between the baseline and FOV.

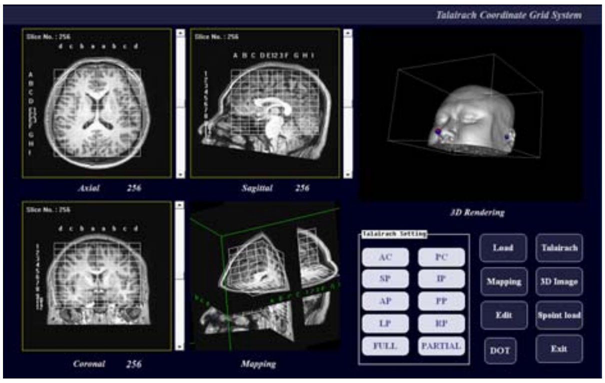

Fig. 12 Registration application to align image coordinate in camera with MRI image coordinate

Figure 12 shows a program for registering the three-dimensional image coordinate of a patient through magnetic resonance imaging and the location coordinate through marker recognition of an infrared camera as the actual TMS navigation software. This program shows registration between the three-dimensional model of magnetic resonance imaging and a patient's head by inducing the location coordinate through camera calibration and undistortion as well as analytical forward intersection.

This study is expected to have a great influence on deciding on FOV and the errors of the three-dimensional coordinate through application to a TMS navigation system. It is ultimately expected to help functional analysis of the brain by applying magnetic stimulation to a correct anatomical location and be helpful in the brain stimulation material field dealing with anatomical research of individual patients with brain function disorder and the research on rehabilitative effects based on location.

Acknowledgments

This study was supported by a grant of the Korea Healthcare technology R&D project, Ministry for Health, Welfare & Family Affairs, Republic of Korea (A101901).

References

[1] "Korean Women's Health Conditions and Policy Agenda", Korean Women's Development Institute, http://www.kwdi.re.kr, accessed Dec. 20. 2011.
[2] A. T. Barker, R. Jalinous, I. L. Freeston, "Noninvasive magnetic stimulation of human motor cortex", Lancet1, pp.1106-1107, 1985.
[3] J. Liepert, H. Bauder, H.R. Wolfgang, W.H. Miltner, E . Taub, C. Weiller, "Treatment-induced cortical reorganization after stroke in humans", Stroke, vol.31, pp.1210-1216, 2000
[4] J. Mally, T.W. Stone, "Improvement in Parkinsonian symptoms after repetitive transcranial magnetic stimulation", journal of the Neurological Sciences, vol.162, no.2, pp.179-184, 1999
[5] U. Herwig, C. Schönfeldt-Lecuona, A. P. Wunderlich, C. von Tiesenhausen, A. Thielscher, H. Walter, M. Spitzer, "The navigation of transcranial magnetic stimulation", PsychiatryResearch: NeuroimagingSection, vol.108, no.2, pp.123-131, 2001.
[6] P. Julkunen, L. Säisänen, N. Danner, E. Niskanen, T. Hukkanen, E. Mervaala, M. Könönen, "Comparison of navigated and non-navigated transcranial magnetic stimulation for motor cortex mapping, motor threshold and motor evoked potentials", NeuroImage, vol.44, no.3, pp.790-795, 2009
[7] Q. Noirhomme, M. Ferrant, Y. Vandermeeren, E. Olivier, B. Macq, O. Cuisenaire, "Registration and Real-Time Visualization of Transcranial Magnetic Stimulation With 3-D MR Images", IEEE Transactios on Biomedical Engineering, vol.51, no.11, pp.1994-2005, 2004
[8] S.G. Mark, A.J. Gary, "Noninvasive techniques for probing neurocircuitry and treating illness: vagus nerve stimulation (VNS), transcranial magnetic stimulation (TMS) and transcranial direct current stimulation (tDCS)", Neuropsychopharmacology, vol.35 , no.1 , pp.301-316 , 2010
[9] J.S. Jung, J.M. Park, B.G. Kim, "Tracking of Moving Objects for Mobile Mapping System", The Journal of GIS Association of Korea, vol.14, no.2, pp.235-244, 2006
[10] Z. Zhang, "A Flexible New Technique for Camera Calibration", IEEE Transactions on Pattern Analysis and Machine Intelligence, vol. 22, no. 11, pp. 1330-1334, 2000
[11] P. Wolf, B.A. Dewitt, Elements of photogrammetry with application in GIS, McGraw-Hill, Ohio, 2000
[12] D. Brown, "Decentering distortion of lenses" , Photogrammetric Eng, vol.32, no.3, pp.444-462, 1966.
[13] K.S. Lee, H.S. Kang, "Calibration Method for Omnidirectional Stereo Camera with Large Baseline", vol.10, no.6, pp.10-17, 2010

Se-jong Ahn received the B.S. degrees in Computer Engineering from Korea Polytechnic University, Siheung, Korea, in 2010 respectively. He has been received the M.S. course in Computer Engineering from Korea Polytechnic University, Siheung , Korea from 2010. His research interests are in image processing, and biomedical signal processing.

Sung-wook Sin received the B.S. degrees in Computer Engineering from Korea Polytechnic University, Siheung, Korea, in 2011 respectively. He has been received the M.S. course in Computer Engineering from Korea Polytechnic University, Siheung , Korea from 2011. His research interests are in image processing, and biomedical signal processing

Hyu-jeong Kim received the B.S., M.S. and Ph.D. degrees in electrical engineering from Kwangwoon University, Seoul, Korea, in 1996, 1999 and 2003, respectively. He is a research professor of Korea Polytechnic University. His research interests include the Computer Engineering and Image Processing

Se-jin Yoon received the B.S.,M.S., and Ph. D. degrees in Medical Engineering from Inje University, Gimhae, Korea,in 1999, 2001, and 2008, respectively. He was a researcher in CR Technology, Daejon, Korea. He is currrently chief research engineer in CR Technology company. Daejeon, Korea. His research interests include rTMS(Transcranial Magnetic Stimulation) and Medical Equipment for rehabilitation

Sung-taek Chung received the B.S., M.S. and Ph.D. degrees in electrical engineering from KAIST, Daejeon, Korea, in 1992, 1995, and 2000 respectively. After graduation, he worked as an R&D Engineer at Medinus Co. (Korea) until 2003. In 2004, he moved to the Korea Polytechnic University (Korea) as a professor of Computer Engineering, and his research interest is in image processing, and biomedical signal processing.